Pseudomonas aeruginosa triggers CFTR-mediated airway surface liquid secretion in swine trachea

Xiaojie Luan[a], Verónica A. Campanucci[a], Manoj Nair[a], Orhan Yilmaz[a], George Belev[b], Terry E. Machen[c], Dean Chapman[d], and Juan P. Ianowski[a,1]

[a]Department of Physiology, University of Saskatchewan, Saskatoon, SK, Canada S7N 5E5; [b]Canadian Light Source Inc., Saskatoon, SK, Canada S7N 2V3; [c]Department of Molecular and Cell Biology, University of California, Berkeley, CA 94720; and [d]Department of Anatomy and Cell Biology, University of Saskatchewan, Saskatoon, SK, Canada S7N 5E5

Edited by James M. Tiedje, Michigan State University, East Lansing, MI, and approved July 16, 2014 (received for review April 9, 2014)

Cystic fibrosis (CF) is an autosomal recessive genetic disorder caused by mutations in the gene encoding for the anion channel cystic fibrosis transmembrane conductance regulator (CFTR). Several organs are affected in CF, but most of the morbidity and mortality comes from lung disease. Recent data show that the initial consequence of CFTR mutation is the failure to eradicate bacteria before the development of inflammation and airway remodeling. Bacterial clearance depends on a layer of airway surface liquid (ASL) consisting of both a mucus layer that traps, kills, and inactivates bacteria and a periciliary liquid layer that keeps the mucus at an optimum distance from the underlying epithelia, to maximize ciliary motility and clearance of bacteria. The airways in CF patients and animal models of CF demonstrate abnormal ASL secretion and reduced antimicrobial properties. Thus, it has been proposed that abnormal ASL secretion in response to bacteria may facilitate the development of the infection and inflammation that characterize CF airway disease. Whether the inhalation of bacteria triggers ASL secretion, and the role of CFTR, have never been tested, however. We developed a synchrotron-based imaging technique to visualize the ASL layer and measure the effect of bacteria on ASL secretion. We show that the introduction of *Pseudomonas aeruginosa* and other bacteria into the lumen of intact isolated swine tracheas triggers CFTR-dependent ASL secretion by the submucosal glands. This response requires expression of the bacterial protein flagellin. In patients with CF, the inhalation of bacteria would fail to trigger ASL secretion, leading to infection and inflammation.

The human airway is normally protected from injury caused by microbial colonization and viral infection by a complex immune defense system. The cornerstone of airway defense is mucociliary clearance. Particles, including bacteria, are captured in mucus and removed by an efficient mucociliary clearance mechanism. Airway host defense is compromised in individuals with cystic fibrosis (CF), whose lungs are thus prone to chronic bacterial infections, frequently with *Pseudomonas aeruginosa,* and inflammation that may eventually cause lung tissue damage and respiratory failure (1, 2). The events leading from cystic fibrosis transmembrane conductance regulator (*CFTR*) gene mutation to airway disease are incompletely understood, but accumulating evidence suggests that CF airway disease results from abnormal microbial clearance (3, 4).

Although chronic inflammation is a major aspect of CF lung disease, recent data show that the initial consequence of CFTR mutation is impaired ability to eradicate bacteria. In previous studies, lungs from animal models of CF (F508del and $CFTR^{-/-}$ pigs) (5, 6) did not eradicate bacteria as effectively as lungs from WT littermates before the development of inflammation (3, 4). These results suggest that impaired bacterial elimination is the pathogenic event that initiates a cascade of inflammation and pathology in CF lungs (4).

The failure to clear bacteria likely results from abnormal airway surface liquid (ASL) secretion and properties (6–10). The ASL consists of a layer of mucus that traps inhaled particles and a periciliary liquid layer that keeps the mucus an optimum distance from the underlying epithelia to maximize ciliary mobility (10, 11). The mucus layer is a complex mixture of water, salts, gel-forming mucins, and antimicrobial compounds that helps inactivate, kill, and trap pathogens and facilitates mucociliary clearance (10, 11). In CF airways, both the bacteria-killing properties and ASL secretion are abnormal (3, 9). The airway liquid produced by $CFTR^{-/-}$ swine has weaker bactericidal properties compared with that produced by WT littermates, owing to abnormal pH (3, 4). In addition, human CF airways, 1-d-old CF piglets, newborn $CFTR^{-/-}$ ferrets, and $CFTR^{-/-}$ mice fail to respond to stimulatory signals that normally elicit strong ASL secretion (6–9). Consequently, it has been proposed that abnormal secretion of fluid and mucin in response to bacterial infection may contribute to the pathogenesis of CF lung disease (7–10, 12–15); however, the central questions of whether bacteria trigger ASL secretion in the airways, and the role of CFTR in such a process, have not been explored previously, owing to the lack of a suitable experimental technique.

We have developed a novel synchrotron-based method to measure the height of the ASL layer covering the epithelium of intact, isolated swine trachea. We show that the introduction of *P. aeruginosa* into the lumen of intact isolated swine tracheas triggers CFTR-dependent ASL secretion by the submucosal glands. This is a local response that affects only the glands in close proximity to the bacteria and requires expression of the bacterial protein flagellin. We also show that *Staphylococcus aureus* and *Haemophilus influenzae* trigger CFTR-dependent

Significance

Cystic fibrosis (CF) is a genetic disorder caused by mutations in the gene encoding for the anion channel cystic fibrosis transmembrane conductance regulator (CFTR). Several organs are affected in CF, but most of the morbidity and mortality comes from lung disease caused by the failure to clear bacteria. Bacterial clearance depends on a layer of airway surface liquid (ASL) covering the airways, rich in antimicrobial compounds and mucins, that removes bacteria from the airway through mucociliary clearance. This study provides the first demonstration that inhalation of bacteria triggers CFTR-dependent ASL secretion. We suggest that this response to inhaled pathogens is an important but previously unknown part of the innate immune response that would be missing in CF patients, resulting in reduced bacterial killing and facilitating infection.

Author contributions: X.L., V.A.C., M.N., G.B., T.E.M., D.C., and J.P.I. designed research; X.L., V.A.C., M.N., O.Y., and J.P.I. performed research; G.B., T.E.M., and D.C. contributed new reagents/analytic tools; X.L., V.A.C., M.N., O.Y., G.B., T.E.M., D.C., and J.P.I. analyzed data; and X.L., V.A.C., T.E.M., D.C., and J.P.I. wrote the paper.

The authors declare no conflict of interest.

This article is a PNAS Direct Submission.

[1]To whom correspondence should be addressed. Email: juan.ianowski@usask.ca.

This article contains supporting information online at www.pnas.org/lookup/suppl/doi:10.1073/pnas.1406414111/-/DCSupplemental.

ASL secretion, indicating that this response is not unique to *P. aeruginosa*. In patients with CF, the inhalation of bacteria would fail to trigger ASL secretion by submucosal glands, facilitating infection and inflammation.

Results and Discussion

Our synchrotron-based method for measuring the height of the ASL layer covering the epithelium lining the lumen of intact, isolated swine trachea makes use of the large difference in the refractive index between the air and the airway liquid layer, which produces a strong signal at the air–liquid interface using phase-contrast imaging (PCI; Fig. 1*A*) (16–19). The position of the tissue was determined using agarose beads (20, 21) that come into direct contact with the surface epithelium (Fig. S1). The height of the ASL layer was measured as the distance between the air–liquid interface and the edge of the agarose beads touching the surface epithelium (Fig. 1*B* and Fig. S1) by a researcher blinded to the experimental conditions. Preliminary experiments showed that beads larger than 100 μm do not migrate during experimentation owing to mucociliary clearance. All of our experiments were performed using beads larger than 200 μm.

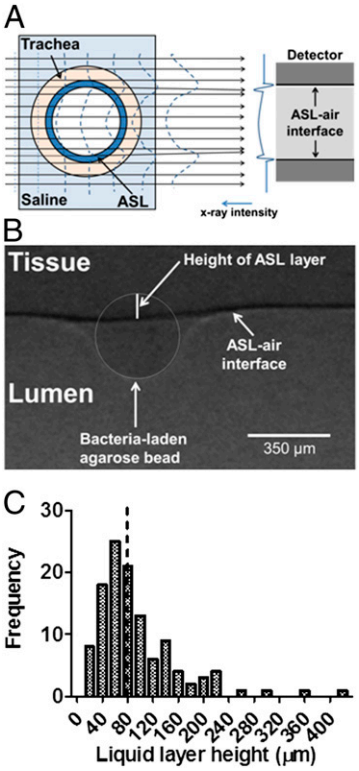

Fig. 1. Synchrotron-based phase contrast imaging. (*A*) Schematic showing the detection of ASL–air interface in the lumen of an intact trachea using PCI. The synchrotron provides a sufficient amount of parallel spatial coherence X-ray to enhance the contrast between air and ASL using PCI. When X-rays pass through the preparation, the difference in refractive index between ASL and air results in a phase shift of X-rays that causes an interference pattern shown on the detector as variations in X-ray intensity. Since the ASL refractive index is very similar to that of the tissue, PCI cannot resolve the ASL–tissue interface. Thus, we use agarose beads to detect the position of the tissue with respect to the ASL–air interface. (*B*) Measurement of ASL height in an intact trachea as the distance between the ASL–air interface (arrow) and the edge of the agarose bead touching the surface epithelium by a researcher blinded to the experimental conditions. The agarose bead sits in the ASL layer, and the border of the agarose bead is highlighted. The distance from the bottom of the agarose bead to ASL–air interface is used to measure the height of the ASL layer. The measured height of the ASL layer in this experiment is 115 μm. (*C*) Frequency distribution and median (dotted line) of ASL height in control tracheas exposed to agar beads containing no bacteria for 5 min; $n = 117$ agarose beads obtained from tracheal preparations from 39 pigs.

The ASL height on the surface of untreated epithelia showed heterogeneity, as reported previously using electron microscopy (22). The height of the ASL layer ranged from 16 to 400 μm, with a median 77 μm (Fig. 1*E*), consistent with previous reports of average ASL heights ranging from 3 to 100 μm depending on species and state of the airway (reviewed in ref. 23).

To test the effect of *P. aeruginosa*, we loaded agarose beads with bacteria and instilled then in the trachea preparation for 35 min. Exposure of the tracheas to bacteria-free agarose beads for 35 min produced a small but significant increase in the height of the ASL (Fig. 2*A*); however, ASL secretion was much greater when tracheas were exposed to *P. aeruginosa*-laden agarose beads (Fig. 2 *B* and *C*). In contrast, tracheal preparations that had been preincubated for 30 min with the CFTR blocker CFTRinh172 (100 μM) failed to respond to *P. aeruginosa* (Fig. 2 *D*–*F*), indicating that *P. aeruginosa* triggered CFTR-dependent ASL secretion in the airways.

Most of the ASL secreted in the upper airways is produced by the submucosal glands, with a smaller contribution from surface epithelium cells (14). To test whether the ASL produced in response to bacteria comes from submucosal glands, we surgically removed the glands from halves of tracheas and compared the ASL secretion with that in the halves containing glands. The tracheal segments containing submucosal glands secreted more fluid in response to *P. aeruginosa* (Fig. 3*A*), indicating that most of the ASL produced in response to bacteria comes from the submucosal glands. Thus, the composition of the ASL secreted in response to *P. aeruginosa* may be similar to that of the fluid secreted by the submucosal glands, containing 94 mM Na^+, 92 mM Cl^-, pH 6.97, and numerous proteins, including mucins, lysozyme, siderocalin, HSC-71, α-1-antitrypsin, and α-1-antichymotrypsin (24, 25).

To test whether the response to the bacteria involved all glands in the preparation or just those in close proximity to the bacteria, we developed a method based on K-edge subtraction (26) that allowed us to distinguish bacteria-laden beads and bacteria-free beads in a preparation (Fig. 3*B*). When we instilled both *P. aeruginosa*-laden and bacteria-free agarose beads in a trachea, the bacteria-laden beads exhibited a much larger increase in ASL height after 35 min of incubation (Fig. 3*C*). These results indicate that the response to *P. aeruginosa* is not a general response affecting all glands, but rather a local response by submucosal glands adjacent to the bacteria (10, 15).

Detection of *P. aeruginosa* by the nasal epithelial cell line CF15 requires the expression of flagellin, an abundant bacterial structural protein (27). Thus, we tested the effect of *P. aeruginosa* mutant strain PAKΔfliC, which lacks flagellin. In contrast to the WT PAK strain, PAKΔfliC failed to stimulate ASL secretion in swine trachea, (Fig. 4*A*). In addition, agarose beads loaded with flagellin produced similar ASL secretion as PAK (Fig. 4*A*). These results suggest that *P. aeruginosa* must express flagellin to stimulate ASL secretion.

The direct addition of flagellin (10 ng/mL) to the serosal side (i.e., in direct contact with the submucosal glands) did not stimulate secretion, whereas addition of the proinflammatory cytokine IL-1β did (50 ng/mL) (Fig. 4*B*). These results suggest that flagellin does not directly stimulate submucosal glands to trigger ASL secretion, but rather may bind to Toll-like receptor 5 (TLR5) in the surface epithelia lining the lumen of the airways and trigger one or more paracrine signals, such as IL-1β, which in turn stimulate submucosal gland ASL secretion (28). Consistent with this hypothesis, RT-PCR detected TLR5 expression in surface epithelia, but not in the submucosal glands (Fig. 4*C*). In addition, RT-PCR showed that submucosal glands express the IL-1β receptor, IL-1R1 (Fig. 4*F*). IL-1R1 immunostaining colocalizes with

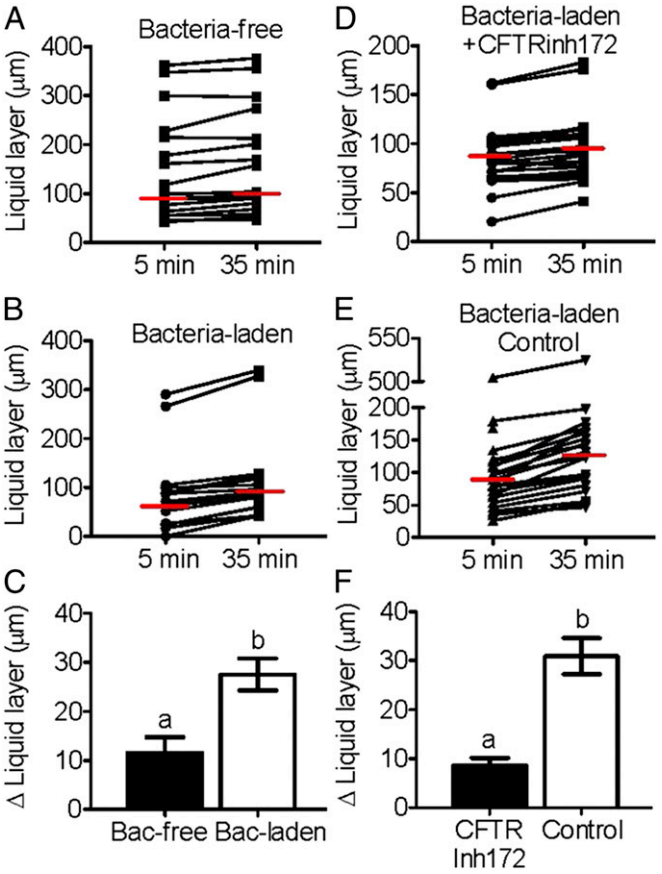

Fig. 2. Bacteria stimulate ASL secretion (*A*–*C*), which is inhibited by CFTRinh172 (*D*–*F*). (*A* and *B*) Scatterplot and median of ASL height in tracheas exposed to bacteria-free (*A*) and *P. aeruginosa*-laden (*B*) agarose beads. The median ASL height increased from 99 μm to 103 μm after a 35-min incubation with bacteria-free agarose beads (n = 18) and from 66 μm to 89 μm after a 35-min incubation with bacteria-laden agarose beads (n = 19) ($P < 0.05$, Wilcoxon signed-rank test). (*C*) Average increase in ASL height triggered by bacteria-laden (n = 19) and bacteria-free (n = 18) agarose beads ($P < 0.05$, Student t test). Columns labeled with different letters differ significantly). (*D*) Scatterplot and median values of ASL heights of tracheal preparations incubated for 30 min with CFTRinh172 (100 μM) before exposure to *P. aeruginosa*-laden agarose beads. The median ASL height did not change after a 35-min incubation with bacteria-laden agarose beads in CFTRinh172-treated preparations (n = 26; $P > 0.05$, Wilcoxon signed-rank test). The cartilage surrounding the trachea was dissected out to ensure access of the blocker. (*E*) Scatterplot and median values of ASL heights of tracheas that underwent the same surgical procedure as tracheas in *D* and before exposure to *P. aeruginosa*-laden agarose beads. The median ASL height increased from 86 μm to 143 μm after a 35-min incubation with bacteria-laden beads (n = 26; $P < 0.05$, Wilcoxon signed-rank test). (*F*) Average increase in ASL height triggered by bacteria-laden beads in CFTRinh172-treated and untreated controls (n = 26 for both CFTRinh172 and controls; $P < 0.05$, Student t test). Columns labeled with different letters differ significantly.

lysozyme, a marker for serous cells that are the driving force for submucosal gland secretion (Fig. 4*E*).

If flagellin does in fact trigger the release of paracrine signals to the submucosa, then these signals should accumulate in the solution bathing the submucosa. To test this hypothesis, we used a modified airway submucosal gland secretion assay preparation with intact surface epithelia. We incubated the surface epithelia with *P. aeruginosa* (PAK or PAKΔfliC) or PBS for 35 min, and then collected the Krebs solution bathing the serosal side of the preparation. We tested the effect of the collected fluid on submucosal gland secretion using a secretion assay. The liquid collected from preparations incubated with PAK stimulated significantly greater submucosal gland secretion compared with the liquid collected from preparations incubated with PAKΔfliC or PBS (Fig. 4*D*). These results suggest that flagellin shed by inhaled *P. aeruginosa* binds TLR5 expressed by the surface epithelium cells (reviewed in ref. 29), triggering the release of proinflammatory cytokines into the submucosa within several minutes (30). The cytokines diffuse from the surface epithelium to the glands located ~150 μm away (31, 32), stimulating CFTR-dependent ASL secretion (13). Flagellin also will induce mucin expression within 18–24 h and further contribute to bacteria clearance (33, 34).

P. aeruginosa is not the only bacteria encountered by CF patients. Other pathogens, such as *S. aureus* and *H. influenzae*, may appear in the airways before *P. aeruginosa*. Thus, we tested whether the airways respond to instillation of *S. aureus*- and *H. influenzae*-laden agarose beads. Our results show that both of these pathogens triggered CFTR-dependent ASL secretion (Fig. 4 *G* and *H*). Interestingly, these bacteria do not express flagellin, suggesting that some other pattern recognition receptor pathways may be involved in triggering CFTR-dependent ASL secretion.

Our results are the first demonstration that bacteria-triggered, CFTR-dependent ASL secretion is part of the normal innate immune response to inhaled bacteria. CFTR is required for normal fluid secretion, which washes mucins and antimicrobial compounds from the submucosal glands into the airway lumen (7–10, 12–15). The loss of CFTR-mediated fluid secretion reduces ASL secretion, supporting the hypothesis that CFTR mutations lead to reduced secretion of antimicrobial compounds and mucins into the airway lumen, facilitating chronic infection and inflammation (3, 6, 35, 36). Eventually the airway undergoes remodeling, including goblet cell hyperplasia, and more severe

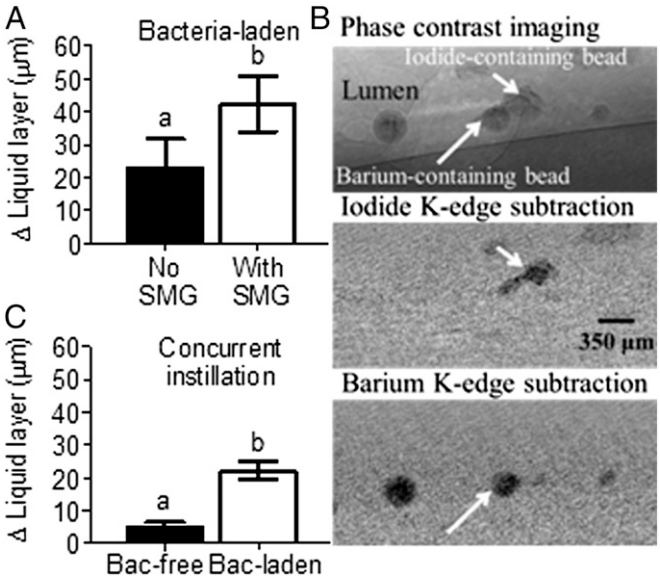

Fig. 3. Submucosal glands are major contributors to bacteria-stimulated ASL secretion. (*A*) Tracheas with submucosal glands (SMG) surgically removed produced less fluid than tracheas with intact SMG (n = 13 with SMG and n = 11 without SMG; $P < 0.05$, Student t test). Columns labeled with different letters differ significantly). (*B*) Bacteria-free and *P. aeruginosa*-laden agarose beads were differentially labeled with barium or iodine and detected using K-edge subtraction. ASL height was measured at each individual bead by a researcher blinded to the experimental conditions. Only bacteria-laden beads showed increases in ASL after a 35-min incubation. On average, there were eight agarose beads per trachea, and the average distance between beads was 1.6 mm. (*C*) Increase in ASL height after a 35-min concurrent instillation of bacteria-free and *P. aeruginosa*-laden agarose beads (n = 23 for both groups; $P < 0.05$, Student t test). Columns labeled with different letters differ significantly.

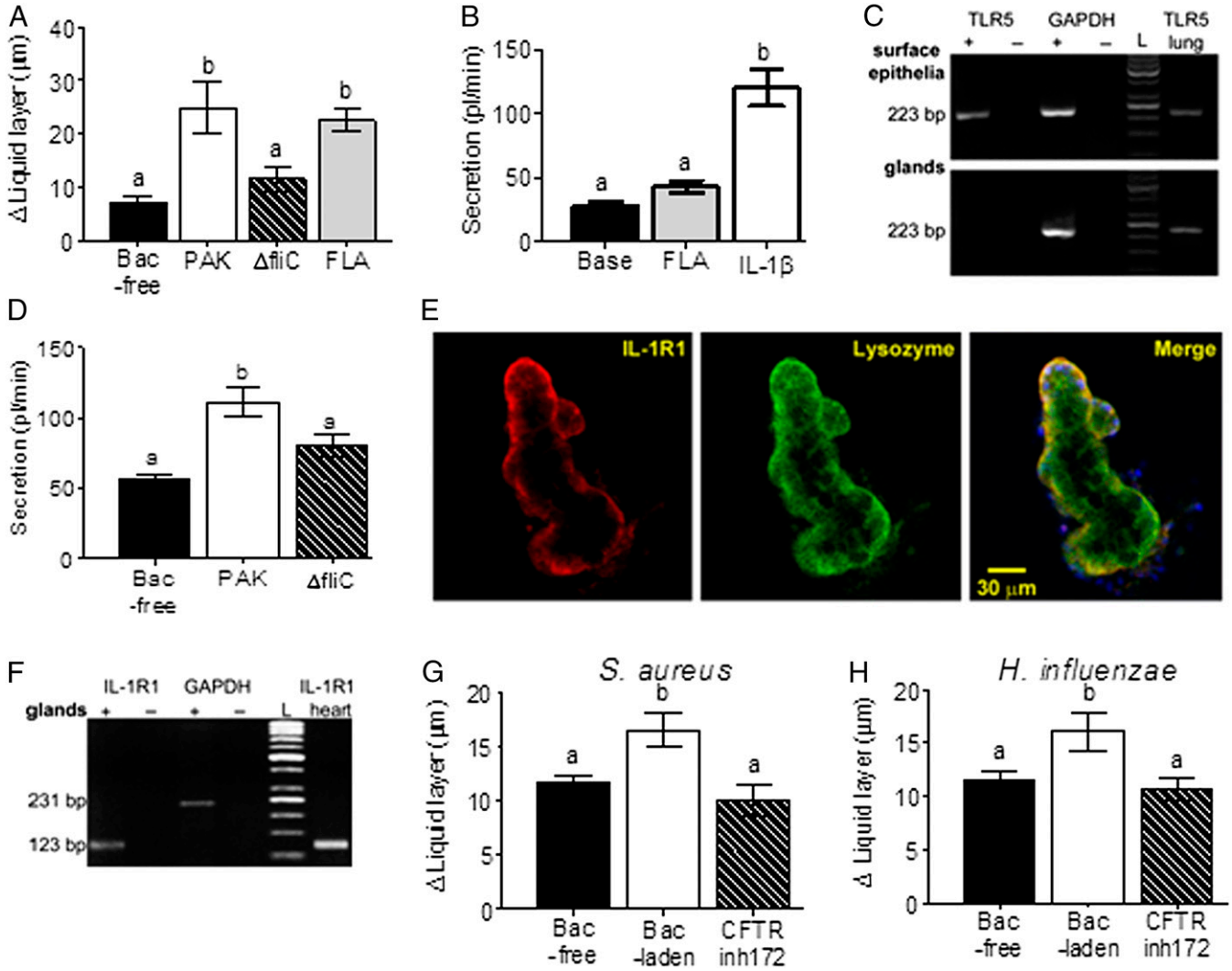

Fig. 4. *P. aeruginosa*-triggered ASL secretion requires expression of flagellin. (*A*) PAKΔfliC-laden agarose beads produced less ASL than PAK-laden agarose beads, and flagellin-laden (10 ng/mL) agarose beads (FLA) triggered a similar response as PAK-laden beads ($n = 12$ bacteria-free, $n = 7$ PAK, $n = 10$ PAKΔfliC, and $n = 15$ FLA; $P < 0.05$, ANOVA and Bonferroni's multiple comparison test). Columns labeled with different letters differ significantly. (*B*) Secretion assay data shows that the addition of flagellin (10 ng/mL) to the Krebs solution bathing the submucosal glands did not stimulate ASL secretion, whereas the addition of IL-1β (50 ng/mL) did ($n = 10$ for flagellin and $n = 9$ for IL-1β; $P < 0.05$, ANOVA and Bonferroni's multiple comparison test). Columns labeled with different letters differ significantly. (*C*) Airway surface epithelia (*Upper*) express the flagellin receptor TLR5, whereas submucosal glands do not (*Lower*). The lung is a positive control for TLR5, and + and − indicate RT positive and negative, respectively. (*D*) The Krebs solution bathing the submucosa of trachea preparations incubated with *P. aeruginosa* strain PAK on the mucosal side stimulated ASL secretion in a secretion assay, whereas PAKΔfliC and PBS did not ($n = 9$ for all groups; $P < 0.05$, ANOVA and Bonferroni's multiple comparison test). Columns labeled with different letters differ significantly. (*E*) Confocal immunofluorescence of IL-1β receptor IL-1R1 (*Left*), lysozyme (*Middle*), and both merged (*Right*) in submucosal glands. The images show that IL-1R1 is colocalized with lysozyme, a marker for serous cells. (*F*) Airway submucosal glands express IL-1R1. The heart is a positive control for IL-1R1, and + and − indicate RT positive and negative, respectively. (*G* and *H*) Bacteria-triggered ASL secretion is not limited to *P. aeruginosa*. Both *S. aureus* (*G*) ($n = 8$ bacteria-free, $n = 10$ *S. aureus*, and $n = 12$ *S. aureus* + CFTRinh172; $P < 0.05$, ANOVA and Bonferroni's multiple comparison test) and *H. influenzae* (*H*) stimulate ASL secretion that is inhibited by CFTRinh172 ($n = 19$ bacteria-free, $n = 11$ *H. influenzae*, and $n = 10$ *H. influenzae* + CFTRinh172; $P < 0.05$, ANOVA and Bonferroni's multiple comparison test). Columns labeled with different letters differ significantly.

pathologies, such as mucus hypersecretion (4). These results suggest that the progression of CF airway disease may be ameliorated by treatments that improve the response of the airways to inhaled bacteria, such as prophylactic antibiotic treatment. In addition, abnormal ASL secretion in response to microbes may contribute to other pathological conditions, such as chronic obstructive pulmonary disease and asthma, in which airway remodeling occurs and responses to microbes could be blunted (37).

Finally, the synchrotron-based technique that we have developed is applicable to living animals (38), making it possible to study the response to bacteria in animal models of CF in vivo and the effect of treatments such as CFTR trafficking correctors.

Materials and Methods

Animals. Tracheas were obtained from juvenile female and male pigs weighing 15–25 kg at the University of Saskatchewan's Prairie Swine Centre. The tracheas were dissected within 15–30 min of euthanasia, clamped at both ends to prevent fluid from entering the trachea, and placed in ice-cold Krebs-Ringer solution containing 115 mM NaCl, 2.4 mM K_2HPO_4, 0.4 mM KH_2PO_4, 1.2 mM $CaCl_2$, 1.2 mM $MgCl_2$, 25 mM $NaHCO_3$, and 10 mM glucose (pH 7.4) equilibrated with 95% O_2, 5% CO_2 until use.

X-Ray Imaging. The experiments were performed on the BioMedical Imaging and Therapy-Bend Magnet beamline 05B1-1 at the Canadian Light Source. All of the experiments were approved by the Canadian Light Source and the University of Saskatchewan's Animal Ethics Committee.

The experimental hutch was located 25.5 m away from the storage ring. PCI was performed using monochromatic 20 keV ($\lambda = 0.062$ nm) X-rays, selected using a standard double-crystal monochromator. Iodine K-edge subtraction imaging was performed using monochromatic 33.09 keV and 33.24 keV. Barium K-edge subtraction imaging was performed using monochromatic 37.37 keV and 37.52 keV. The beam size was 100.0 mm wide × 8.0 mm high. The distance between sample and detector was 65 cm. Images were captured using a high-resolution X-ray converter (AA-60; Hamamatsu Photonics) with a CCD detector (C9300-124; Hamamatsu Photonics). The converter used a 10-μm-thick scintillator (Gd2O2S:Tb) to convert X-rays to visible light, which was then directed to the CCD. The pixel size of the image was 8.75 × 8.75 μm. The exposure time ranged from 600 to 900 ms.

The trachea preparation was placed in a custom-built chamber. The tissue was immersed in Krebs solution plus 1 μM indomethacin at 35 °C and equilibrated with 95% O_2, 5% CO_2. The lumen of the trachea preparation remained free of solution and sealed, but was accessible to the researchers to introduce the agarose beads. Agarose beads, ∼200–800 μm in diameter, were blotted dry and placed in the lumen of the preparation using a cotton swab. Before ASL height measurements, each bead was placed at the point where the ASL-air interface is parallel to the X-rays reaching the sample, that is, the top or bottom of the preparation (Fig. 1*A*), using a computerized experimental stage. Two ASL height measurements were obtained, one at 5 min after instillation of the beads and another at 35 min after instillation. For our experiments, the measurements made at 5 min should be interpreted as the initial state of the airway, that is, before exposure to bacteria. We labeled the first time point as 5 min because there was a 5-min delay between instillation of the beads and acquisition of the first image.

Preparation of Agarose Beads. Agarose beads were used to measure the height of the ASL (Fig. S1). The height of the ASL layer was measured as the distance between the ASL-air interface and the edge of the agarose bead touching the surface epithelia (Fig. S1).

Agarose beads were prepared in sterile conditions with 4% (wt/vol) agarose in PBS as described elsewhere (20, 21). To make the beads visible by X-ray, we added 1 M $BaSO_4$ or CuI as a contrast agent. These salts were chosen because they are not soluble in water and thus do not contribute to the osmotic pressure of the beads. The osmolarity was 278 ± 0.1 mOsm for PBS, 276 ± 0 mOsm for 1 M $BaSO_4$, and 279 ± 0 mOsm for 1 M CuI ($n = 6$ per group).

The agarose beads also served as a delivery system for bacteria to the airways. Bacteria-laden agarose beads were prepared by adding 10% (vol/vol) of bacteria stock solution to sterile PBS. *P. aeruginosa* stock solution was prepared with a *P. aeruginosa* clinical isolate generously provided by Dr. Gordon, University of Saskatchewan (NH57388) (39). An aliquot of *P. aeruginosa* NH57388 was inoculated in 80 mL of TSB in a 2-L Erlenmeyer flask and incubated for 28 h at 37 °C with shaking at 170 rpm. The culture was heat-killed (i.e., incubated at 80 °C for 30 min) and then stored at −20 °C until use. Clinical isolates of *H. influenzae* and *S. aureus* (generously provided by Dr. Blondeau, Royal University Hospital, Saskatoon) and *P. aeruginosa* strains PAK and PAKΔfliC were prepared in an identical manner.

Secretion Assay. A small piece of trachea was cut along the trachealis muscle, and the airway submucosa, containing the glands, was dissected from the cartilage as described previously (40). This submucosa preparation was placed in a custom-built chamber with the serosal side bathed in Krebs solution containing 1 μM indomethacin. The mucosal side was cleaned, dried with a stream of air, and then coated with ∼5 μL of mineral oil. Mucus secreted by the submucosal glands formed a spherical droplet under the mineral oil. The preparation was maintained at 37 °C and equilibrated with warm and humidified 95% O_2, 5% CO_2 gas (TC-102; Medical Systems Corp.). Flagellin (10 ng/mL) was added to the serosal side, and the droplets of ASL secreted by the glands were imaged every 120 s and stored for offline analysis using ImageJ 1.43u. The volumes of the secreted droplets were calculated assuming a spherical shape ($V = 4/3\pi r^3$) (30). The secretion rate was calculated by fitting the volume-versus-time plots with straight lines using linear regression, and the slopes were taken as the secretion rates using at least four points (41).

A modified secretion assay was used to test whether bacteria stimulated the release of paracrine signals that may trigger ASL secretion. For this assay, a piece of trachea was prepared as described above, except that the mucosal side was not cleaned or dried. Instead, the mucosal side of the preparation was incubated with ∼5 μL of PBS or *P. aeruginosa* stock solution. After 35 min, the Krebs solution bathing the serosal side of the preparation was collected and tested using the secretion assay as described above.

Surgical Removal of Submucosal Glands. The tracheal preparation was clamped at both ends so that the lumen was filled with air. The cartilage was removed with the aid of a scalpel and a blunt-ended elevator. Once the cartilage was removed, the submucosal glands and other tissue in the submucosa was dissected out by "shaving" with a breakable scalpel blade (Fine Science Tools). This procedure took ∼30 min. We tested the effectiveness of our procedure by performing it in a set of tracheas and then counting the number of viable glands in a secretion assay. We compared the number of viable glands in tracheas with glands removed and in control tracheas subjected to the same procedure but without gland removal. According to the data, our procedure allowed us to remove 90% of glands from the trachea.

The surface epithelium was not affected by the dissection procedure. During gland dissection, the trachea remained filled with air and clamped on both ends. The dissection tools never touched the surface epithelia. We tested the condition of the surface epithelium after dissection of submucosal glands by measuring short circuit currents in an Ussing chamber. The experiments showed that preparations subjected to the dissection procedure (removal of the cartilage) but with submucosal glands intact had a short circuit current (I_{sc}) of 24 μA/cm^2. Similarly, preparations in which the glands were dissected out had an I_{sc} of 20 μA/cm^2. The addition of amiloride (10^{-4} M apical side) reduced the I_{sc} to 12 μA/cm^2 for preparations with glands and 9 μA/cm^2 for preparations without glands. Stimulation with forskolin (10^{-5} M apical side) stimulated I_{sc} to 20 μA/cm^2 for preparations with glands and to 17 μA/cm^2 for preparations without glands. These results show that the surface epithelium was not affected by the dissection procedure.

RT-PCR. Total RNA was extracted from 10–20 mg of tissue (surface epithelia, submucosal glands, heart, and lung) using an RNAqueous Kit (Ambion). Airway surface epithelium was dissected from swine trachea and was free of submucosal glands. Submucosal glands were individually dissected and cleaned of connective tissue. RNA was reverse-transcribed with cells-to-cDNA II Kit (Ambion) and amplified using Platinum II Taq DNA Polymerase (Invitrogen) using the following gene-specific primers: TLR5 (AB208697): 5′-GGCCATAGTCAGATCGCATTCTTGC-3′ and 5′-GATCAATGGCCTTCAAGGAATTCAG-3′, amplicon size 223 bp (42); IL-1R1 (XM005662366): 5′-ACGGGTCCACCTCTAACTCA-3′ and 5′-CAGCAATGCTTTCCCCAACG-3′, amplicon size 123 bp; and GAPDH (AF017079): 5′-GATGGTGAAGGTCGGAGTGAACGG-3′and 5′-CCTGGAAGATGGTGATGGGATTTCC-3′, amplicon size 231 bp (32). The annealing temperature was 58 °C. Negative controls were performed by omitting the Moloney murine leukemia virus reverse-transcriptase enzyme (Ambion) in the reverse-transcription reaction or omitting the input cDNA in the PCR. The positive control was lung parenchyma for TLR5 (32) and heart muscle for IL-1R1 (43). PCR was held at 94 °C for 2 min and cycled 40 times. Each cycle consisted of 94 °C for 30 s (denaturation), 58 °C for 30 s (annealing), and 72 °C for 1 min (extension). This was followed by a 10-min final extension at 72 °C. PCR products were visualized on an ethidium bromide-stained 2% (wt/vol) agarose gel under UV illumination. The PCR product was extracted from the gel and sequenced (Pure Link Gel Extraction Kit; Invitrogen). The amplified product matched the DNA sequence for TLR5 and IL-1R1 from *Sus scrofa* BLAST database.

Confocal Immunofluorescence. Freshly dissected submucosal glands from pig tracheas were fixed in 4% (wt/vol) paraformaldehyde overnight at 4 °C. After three 5-min washes in PBS, submucosal glands were incubated with antibodies for confocal immunofluorescence. The following antibodies were applied sequentially: polyclonal rabbit antibody anti-human (pig reactive) lysozyme (Lyz, 12 mg/L; Abcam) applied overnight at 4 °C; FITC-conjugated secondary antibody against rabbit (1:100; Abcam) applied for 1 h at room temperature; polyclonal rabbit anti-human (pig reactive) IL-1R1 (1:100; Santa Cruz Biotechnology) applied for 1 h at 37 °C; and Texas Red-conjugated secondary antibody against rabbit (1:100; Abcam) applied for 1 h at room temperature. Antibodies were diluted in PBS containing 1% BSA (Sigma-Aldrich) and 0.5% Triton X-100 (Sigma-Aldrich). After each incubation, the samples underwent three 5-min washings in PBS. Samples were covered with the anti-photobleaching mounting medium (Vectashield with DAPI; Vector Laboratories) and then viewed with a confocal microscope (LSM 510 Confor 2; Carl Zeiss) equipped with diode (405 nm), argon (488 nm), and helium/neon (543 nm) lasers. Tissue was scanned in optical sections using Zeisss LSM510/ConfoCor2 version 3.2 SP2 software. In control experiments, either preincubation with blocking peptide or omission of the primary antibody resulted in complete abolition of staining. In control experiments, blocking peptide for IL-1R1 (Santa Cruz Biotechnology) was preincubated with primary antibody (5 μg peptide/1 μg antibody) overnight at 4 °C before application. Image processing was performed with Adobe Photoshop CS5 software.

Reagents. CFTRinh172, IL-1β, and flagellin from *Salmonella typhimurium* were obtained from Cedarlane Labs. A stock solution of CFTRinh172 was dissolved in DMSO. The final concentration of DMSO was <0.1%. The solutions of IL-1β and flagellin were dissolved directly in Krebs solution.

Statistics. Datasets displaying normal distribution are presented as mean ± SEM, whereas other datasets are presented as median and scatterplot. The data were tested for normality using the Kolmogorov–Smirnov test, and the variances were tested using the F test for unequal variances. Those datasets showing normal distributions and similar variances were analyzed using the Student *t* test or ANOVA as appropriate. Other datasets were analyzed using the nonparametric paired sample Wilcoxon signed-rank test. Statistical analyses was performed with GraphPad Prism 5. All analyses were two-tailed, and differences were considered significant at $P < 0.05$.

ACKNOWLEDGMENTS. We thank Drs. Adam Webb and Tomasz Wysokinsk for assistance in developing the synchrotron-based imaging technique; Drs. Baljit Singh, Nigel West, and Michel Desautels for their comments; and Landon Baillie and Dr. Sean Mulligan for assisting with imaging. X.L. was supported by a Canadian Institutes of Health Research-Thrust fellowship. This work was funded by a Cystic Fibrosis Canada grant (to J.P.I.) and a Discovery grant from the Natural Sciences and Engineering Research Council of Canada (to V.A.C.).

1. Pilewski JM, Frizzell RA (1999) Role of CFTR in airway disease. *Physiol Rev* 79(1, Suppl): S215–S255.
2. Sheppard DN, Welsh MJ (1999) Structure and function of the CFTR chloride channel. *Physiol Rev* 79(1, Suppl):S23–S45.
3. Pezzulo AA, et al. (2012) Reduced airway surface pH impairs bacterial killing in the porcine cystic fibrosis lung. *Nature* 487(7405):109–113.
4. Stoltz DA, et al. (2010) Cystic fibrosis pigs develop lung disease and exhibit defective bacterial eradication at birth. *Sci Transl Med* 2(29):29ra31.
5. Rogers CS, et al. (2008) The porcine lung as a potential model for cystic fibrosis. *Am J Physiol Lung Cell Mol Physiol* 295(2):L240–L263.
6. Sun X, et al. (2010) Disease phenotype of a ferret CFTR-knockout model of cystic fibrosis. *J Clin Invest* 120(9):3149–3160.
7. Ianowski JP, Choi JY, Wine JJ, Hanrahan JW (2007) Mucus secretion by single tracheal submucosal glands from normal and cystic fibrosis transmembrane conductance regulator knockout mice. *J Physiol* 580(Pt 1):301–314.
8. Joo NS, Cho HJ, Khansaheb M, Wine JJ (2010) Hyposecretion of fluid from tracheal submucosal glands of CFTR-deficient pigs. *J Clin Invest* 120(9):3161–3166.
9. Joo NS, et al. (2002) Absent secretion to vasoactive intestinal peptide in cystic fibrosis airway glands. *J Biol Chem* 277(52):50710–50715.
10. Wine JJ (2007) Parasympathetic control of airway submucosal glands: Central reflexes and the airway intrinsic nervous system. *Auton Neurosci* 133(1):35–54.
11. Knowles MR, Boucher RC (2002) Mucus clearance as a primary innate defense mechanism for mammalian airways. *J Clin Invest* 109(5):571–577.
12. Martens CJ, et al. (2011) Mucous solids and liquid secretion by airways: Studies with normal pig, cystic fibrosis human, and non-cystic fibrosis human bronchi. *Am J Physiol Lung Cell Mol Physiol* 301(2):L236–L246.
13. Baniak N, Luan X, Grunow A, Machen TE, Ianowski JP (2012) The cytokines interleukin-1β and tumor necrosis factor-α stimulate CFTR-mediated fluid secretion by swine airway submucosal glands. *Am J Physiol Lung Cell Mol Physiol* 303(4): L327–L333.
14. Reid L (1960) Measurement of the bronchial mucous gland layer: A diagnostic yardstick in chronic bronchitis. *Thorax* 15:132–141.
15. Ianowski JP, Choi JY, Wine JJ, Hanrahan JW (2008) Substance P stimulates CFTR-dependent fluid secretion by mouse tracheal submucosal glands. *Pflugers Arch* 457(2): 529–537.
16. Lewis RA, et al. (2005) Dynamic imaging of the lungs using X-ray phase contrast. *Phys Med Biol* 50(21):5031–5040.
17. Morgan KS, et al. (2013) Measuring airway surface liquid depth in ex vivo mouse airways by x-ray imaging for the assessment of cystic fibrosis airway therapies. *PLoS ONE* 8(1):e55822.
18. Parsons DW, et al. (2008) High-resolution visualization of airspace structures in intact mice via synchrotron phase-contrast X-ray imaging (PCXI). *J Anat* 213(2):217–227.
19. Siu KK, et al. (2008) Phase contrast X-ray imaging for the non-invasive detection of airway surfaces and lumen characteristics in mouse models of airway disease. *Eur J Radiol* 68(3, Suppl):S22–S26.
20. Cash HA, Woods DE, McCullough B, Johanson WG, Jr, Bass JA (1979) A rat model of chronic respiratory infection with *Pseudomonas aeruginosa*. *Am Rev Respir Dis* 119(3): 453–459.
21. Chmiel JF, Konstan MW, Berger M (2002) Murine models of CF airway infection and inflammation. *Methods Mol Med* 70:495–515.
22. Sims DE, Horne MM (1997) Heterogeneity of the composition and thickness of tracheal mucus in rats. *Am J Physiol* 273(5 Pt 1):L1036–L1041.
23. Worthington EN, Tarran R (2011) Methods for ASL measurements and mucus transport rates in cell cultures. *Methods Mol Biol* 742:77–92.
24. Jayaraman S, Joo NS, Reitz B, Wine JJ, Verkman AS (2001) Submucosal gland secretions in airways from cystic fibrosis patients have normal [Na(+)] and pH but elevated viscosity. *Proc Natl Acad Sci USA* 98(14):8119–8123.
25. Joo NS, Lee DJ, Winges KM, Rustagi A, Wine JJ (2004) Regulation of antiprotease and antimicrobial protein secretion by airway submucosal gland serous cells. *J Biol Chem* 279(37):38854–38860.
26. Rubenstein E, et al. (1986) Transvenous coronary angiography in humans using synchrotron radiation. *Proc Natl Acad Sci USA* 83(24):9724–9728.
27. Hybiske K, Ichikawa JK, Huang V, Lory SJ, Machen TE (2004) Cystic fibrosis airway epithelial cell polarity and bacterial flagellin determine host response to *Pseudomonas aeruginosa*. *Cell Microbiol* 6(1):49–63.
28. Illek B, et al. (2008) Flagellin-stimulated Cl^- secretion and innate immune responses in airway epithelia: Role for p38. *Am J Physiol Lung Cell Mol Physiol* 295(4):L531–L542.
29. Lambrecht BN, Hammad H (2012) The airway epithelium in asthma. *Nat Med* 18(5): 684–692.
30. Reiniger N, et al. (2007) Resistance to *Pseudomonas aeruginosa* chronic lung infection requires cystic fibrosis transmembrane conductance regulator-modulated interleukin-1 (IL-1) release and signaling through the IL-1 receptor. *Infect Immun* 75(4): 1598–1608.
31. Kreda SM, et al. (2005) Characterization of wild-type and deltaF508 cystic fibrosis transmembrane regulator in human respiratory epithelia. *Mol Biol Cell* 16(5): 2154–2167.
32. Ostedgaard LS, et al. (2011) The ΔF508 mutation causes CFTR misprocessing and cystic fibrosis-like disease in pigs. *Sci Transl Med* 3(74):74ra24.
33. Ben Mohamed F, et al. (2012) A crucial role of Flagellin in the induction of airway mucus production by *Pseudomonas aeruginosa*. *PLoS ONE* 7(7):e39888.
34. Li JD, et al. (1998) Activation of NF-kappaB via a Src-dependent Ras-MAPK-pp90rsk pathway is required for *Pseudomonas aeruginosa*-induced mucin overproduction in epithelial cells. *Proc Natl Acad Sci USA* 95(10):5718–5723.
35. Cho HJ, Joo NS, Wine JJ (2011) Defective fluid secretion from submucosal glands of nasal turbinates from $CFTR^{-/-}$ and CFTR ($^{\Delta F508/\Delta F508}$) pigs. *PLoS ONE* 6(8):e24424.
36. Meyerholz DK, Stoltz DA, Pezzulo AA, Welsh MJ (2010) Pathology of gastrointestinal organs in a porcine model of cystic fibrosis. *Am J Pathol* 176(3):1377–1389.
37. Matkovic Z, Miravitlles M (2013) Chronic bronchial infection in COPD: Is there an infective phenotype? *Respir Med* 107(1):10–22.
38. Luan X, Chapman D, Ianowski JP (2013) Novel method to observe the mucus layer in the living swine using synchrotron-based phase contrast imaging. *Pediatr Pulmonol* S36:239.
39. Hoffmann N, et al. (2005) Novel mouse model of chronic *Pseudomonas aeruginosa* lung infection mimicking cystic fibrosis. *Infect Immun* 73(4):2504–2514.
40. Joo NS, Wu JV, Krouse ME, Saenz Y, Wine JJ (2001) Optical method for quantifying rates of mucus secretion from single submucosal glands. *Am J Physiol Lung Cell Mol Physiol* 281(2):L458–L468.
41. Joo NS, Saenz Y, Krouse ME, Wine JJ (2002) Mucus secretion from single submucosal glands of pig: Stimulation by carbachol and vasoactive intestinal peptide. *J Biol Chem* 277(31):28167–28175.
42. Shinkai H, et al. (2006) Biased distribution of single nucleotide polymorphisms (SNPs) in porcine Toll-like receptor 1 (TLR1), TLR2, TLR4, TLR5, and TLR6 genes. *Immunogenetics* 58(4):324–330.
43. Zitta K, et al. (2010) Interleukin-1beta regulates cell proliferation and activity of extracellular matrix remodelling enzymes in cultured primary pig heart cells. *Biochem Biophys Res Commun* 399(4):542–547.
44. Lee WL, et al. (2011) Muco-ciliary transport: Effect of mucus viscosity, cilia beat frequency and cilia density. *Comput Fluids* 49(1):214–221.